Anisotropic Melting of Frustrated Ising Antiferromagnets

Matthew W. Butcher,[1] Makariy A. Tanatar,[2,3] and Andriy H. Nevidomskyy[1,*]
[1]Department of Physics and Astronomy, Rice University, Houston Texas 77005, USA
[2]Ames National Laboratory, Ames, Iowa 50011, USA
[3]Department of Physics and Astronomy, Iowa State University, Ames, Iowa 50011, USA

(Received 31 December 2021; revised 23 May 2022; accepted 2 March 2023; published 19 April 2023)

Magnetic frustrations and dimensionality play an important role in determining the nature of the magnetic long-range order and how it melts at temperatures above the ordering transition T_N. In this Letter, we use large-scale Monte Carlo simulations to study these phenomena in a class of frustrated Ising spin models in two spatial dimensions. We find that the melting of the magnetic long-range order into an isotropic gaslike paramagnet proceeds via an intermediate stage where the classical spins remain anisotropically correlated. This correlated paramagnet exists in a temperature range $T_N < T < T^*$, whose width increases as magnetic frustrations grow. This intermediate phase is typically characterized by short-range correlations; however, the two-dimensional nature of the model allows for an additional exotic feature—formation of an incommensurate liquidlike phase with algebraically decaying spin correlations. The two-stage melting of magnetic order is generic and pertinent to many frustrated quasi-2D magnets with large (essentially classical) spins.

DOI: 10.1103/PhysRevLett.130.166701

The formation of long-range magnetic order (LRO) upon cooling from a disordered paramagnetic (PM) phase is akin to a gas-to-solid transition. The "solid" phase is characterized by a spontaneously broken symmetry with long-range order in the spin-spin correlations. Studies of geometric frustrations and their effect on this transition have a long history—it is well established that frustrations suppress the Néel transition temperature T_N relative the Curie-Weiss temperature, which is often quantified by the Ramirez frustration ratio $\eta = T_{CW}/T_N$ [1]. In some highly frustrated lattices, such as the corner-sharing tetrahedra in pyroclore magnets [2] or corner-sharing triangles in kagomé compounds [3,4], T_N is suppressed to zero, with the formation of a (classical [5] or quantum [6]) spin liquid and associated order-by-disorder lifting of the extensive ground state degeneracy [7]. However, highly frustrated geometries are not the only way to suppress LRO. Instead, one may consider seemingly simple bipartite lattices, such as the square or cubic lattice systems with competing spin interactions between the nearest and farther neighbors (a paradigmatic $J_1 - J_2$ model on a square lattice is one such example [8]). Apart from suppressing the Néel temperature, do such interaction-induced frustrations affect the process of "melting" of the LRO when the ground state is not extensively degenerate? Furthermore, what is the role of the dimensionality of the magnetic system—which can be controlled in principle by tuning the degree of anisotropy of the exchange interactions along the different crystal directions—on the strength of thermal fluctuations?

In this Letter, we perform Monte Carlo simulations to study a *classical* magnet with anisotropic interactions to elucidate the effect of both the anisotropy and magnetic frustrations on the process by which the magnetically ordered "solid" melts. Our key finding is that this melting proceeds via an intermediate stage in a range of temperatures above the Néel ordering temperature T_N, where the correlations between the spins remain significant and retain the "knowledge" of the anisotropy present in the Hamiltonian. This intermediate correlated paramagnet (CPM) eventually undergoes a crossover into a more conventional paramagnet at a temperature $T^* > T_N$, above which the correlation length is of the order of the lattice constant, and the anisotropy is lost. We find that the dynamic temperature range of this CPM, $\Delta T = T^* - T_N$, grows with increasing frustrations, and that the CPM occupies a significant portion of the phase diagram even as T_N is suppressed to zero by frustrations. These classical results are relevant to many experimental systems (both itinerant and insulating magnets) with large magnetic moments that can be treated as classical, where the evidence of the crossover scale T^* and the anisotropic CPM has accumulated, for instance in Eu-based helimagnets [9–12], some heavy fermion compounds with helical order [13–15], in layered ferromagnets [16], and at a field-tuned quantum critical point in $CeCoIn_5$ [17–19].

Model.—The three-dimensional (3D) anisotropic next-nearest neighbor Ising (ANNNI) model, with ferromagnetic interactions in the plane and competing interactions along the c axis of hexagonal crystal, was first proposed by Elliot [20] to explain complex helicoidal orders and their temperature evolution in the rare-earth magnets. As we show in this Letter, this uniaxial frustration plays a pivotal role in

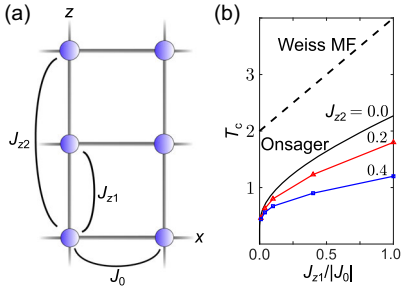

FIG. 1. Suppression of T_N with the addition of frustrating interactions. (a) Diagram of interactions in the 2D ANNNI model. (b) Comparison of T_N from Weiss molecular field theory (dashed line), the Onsager solution ($J_{z2} = 0$, solid black line), and the 2D ANNNI model with $J_{z2} = 0.2J_{z1}$ (red line) and $J_{z2} = 0.4J_{z1}$ (blue line).

how this anisotropic magnet "melts." We consider as our starting point the 2D ANNNI model [Fig. 1(a)]:

$$H = \sum_i [J_0 \sigma_i \sigma_{i+\hat{x}} + J_{z1} \sigma_i \sigma_{i+\hat{z}} + J_{z2} \sigma_i \sigma_{i+2\hat{z}}]. \quad (1)$$

The variables $\sigma_i \in \{-1, 1\}$ are classical Ising spins, with ferromagnetic coupling along the x direction $J_0 < 0$, and competing antiferromagnetic interactions along z: $0 < J_{z2} < J_{z1}$. The reason for our considering a 2D version of the model is both because of its simplicity, and because it evades the entropy-induced multitude of incommensurate phases ("devil's staircase") experimentally found in CeSb [21] and specific to the 3D ANNNI model at finite temperatures [22–29].

First, we consider anisotropy in the absence of frustration, in this case with $J_{z2} = 0$. The Weiss molecular field approach [30] predicts an ordered phase of ferromagnetic chains that are stacked antiferromagnetically in the z direction, occurring below a mean-field critical temperature given by $k_B T_{\mathrm{MF}} = 2(|J_0| + |J_{z1}|)$ [Fig. 1(b), dashed line]. The thermal fluctuations alter this behavior considerably, as famously shown by Onsager [31], resulting notably in the much lower transition temperature T_N than predicted by Weiss molecular-field theory, namely given by the following equation [with $\beta_c = (k_B T_N)^{-1}$]:

$$\sinh(2\beta_c |J_0|) \sinh(2\beta_c |J_{z1}|) = 1. \quad (2)$$

The resulting critical temperature is shown in Fig. 1(b) (solid black line) as a function of the anisotropy J_{z1}/J_0. Notably, as a result of thermal fluctuations, $T_N \to 0$ in the one-dimensional (1D) limit of $J_{z1} \to 0$. This effect bears a striking resemblance to the suppression of T_N in the quantum Heisenberg model in two dimensions, which is itself a consequence of the Mermin-Wagner theorem [32]. The existence and proximity of a lower critical dimension in both the quantum and classical cases is important for the emergence of the anisotropic CPM phase.

Geometric frustrations and anisotropic CPM.—With the addition of geometric frustration in the form of an antiferromagnetic coupling between second-neighbor layers $0 < J_{z2} < J_{z1}/2$, the mean-field energy scale $k_B T_{\mathrm{MF}} = 2(|J_0| + J_{z1} - J_{z2})$ is lowered slightly, whereas the true transition temperature is further suppressed by frustrations as shown in Fig. 1(b) (red and blue lines).

The results for the frustrated 2D ANNNI model were computed using classical Monte Carlo simulation with conventional Metropolis updates, as well as cluster updates, and parallel tempering [33]. By analyzing the spin-spin correlation functions in our Monte Carlo simulations,

$$C(\mathbf{r}) \equiv \langle \sigma(0)\sigma(\mathbf{r}) \rangle \sim f(\mathbf{r}) \cos(qz), \quad (3)$$

we extract the correlation lengths ξ_x and ξ_z from the spatial decay of $f(r) \sim r^{-1/2} \exp[-\sqrt{(x/c)^2 + z^2}/\xi_z]$, where $c = \xi_x/\xi_z > 1$ due to anisotropy. Here the factor $r^{-1/2}$ arises in accordance with the canonical Ornstein-Zernike form for correlations in two dimensions [44]. The data presented below are the results of fits to the functional form, Eq. (3), on finite systems with $L_x = L_z = 64$. Because the correlations in the CPM phase are much shorter than the finite system size ($\xi_x \ll L_x, \xi_z \ll L_z$), finite-size effects will only modify quantitative features such as the precise value of T_N, leaving our primary results unchanged. Data for additional system sizes $L \in \{32, 48, 56, 64, 96, 128\}$ as well as the extended aspect ratio $L_z = 2L_x$ are presented in the Supplemental Material [33].

As expected, we find that the correlation lengths diverge below T_N but are finite and anisotropic above the transition as shown in Fig. 2(b). This resembles the situation in a classical liquid, which has a short-range order (SRO) but no long-range order. However unlike in a classical liquid, spin correlations retain the "memory" of the anisotropy $J_{z1}/J_0 < 1$, with the resulting correlation length being much shorter in the z direction $\xi_z \ll \xi_x$ as shown in Fig. 2(b). One can picture this anisotropic CPM as consisting of oblong droplets of size ξ_x and ξ_z in the lateral and vertical direction, respectively, with the spins correlated within the droplet but not between them [see the insets in Fig. 2(a) for Monte Carlo snapshots]. As the temperature increases, these oblong droplets shrink until eventually their large axis (ξ_x) becomes comparable to the lattice spacing—at that temperature, which we denote by T^*, a crossover into a conventional paramagnet occurs, with very short-ranged correlations in both directions. While magnetic frustrations suppress T_N, the dynamic temperature range $T_N < T < T^*$ where the anisotropic CPM exists grows with increased frustrations, as shown by the color scale in Fig. 2(c). This range becomes especially pronounced when frustration is largest near $J_{z2}/J_{z1} = 1/2$.

Floating "liquid" phase.—The evolution of a CPM into a paramagnet at T^* is a crossover rather than a true phase transition in the regime $J_{z2}/J_{z1} < 1/2$ where the spin

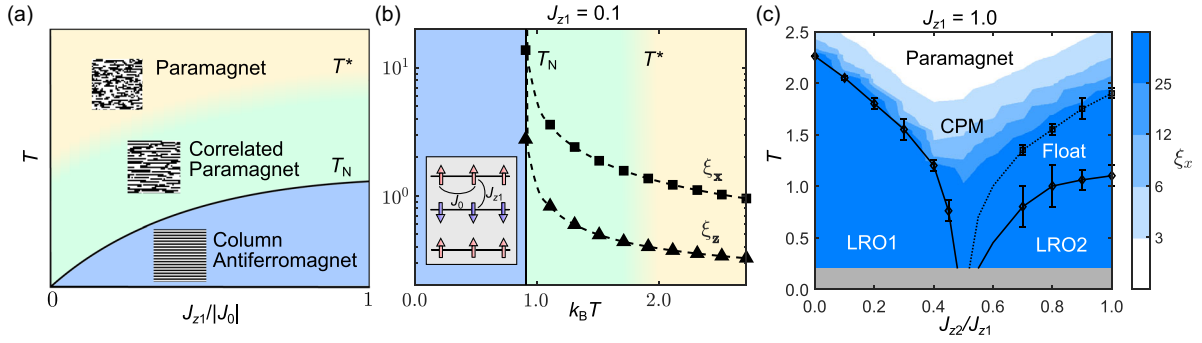

FIG. 2. Schematic diagram (a) demonstrating the concept of anisotropic melting in a 2D Ising system with spatially anisotropic interactions, $0 < J_{z1} < |J_0|$. Insets in (a) are bitmap images of microstates from a Monte Carlo simulation. (b) The correlation lengths ξ_x and ξ_z, fit from the Onsager solution [31,45] for $J_{z1} = 0.1|J_0|$, with ξ_x growing below T^* while ξ_z remains negligible. (c) Contour plot of ξ_x in the 2D ANNNI model for $J_{z1} = |J_0|$. The T^* scale, defined here as the temperature below which ξ_x grows larger than three lattice sites, is most suppressed when approaching the frustration point $J_{z2}/J_{z1} = 0.5$.

correlations remain commensurate with the lattice [$q = Q_1 = \pi$ in Eq. (3)]. Upon further increase of J_{z2}, the correlations in the high-temperature paramagnet become incommensurate, with the value of $\pi/2 < q < \pi$ shown by color in Fig. 3(a). Surprisingly, in this regime the correlated paramagnet acquires a very different character, with spin correlations that decay algebraically while oscillating with an incommensurate wave vector $q = \pi/2 + \Delta q$:

$$C_{\text{float}}(r) \sim \frac{1}{r^{\eta}} \cos(qz), \tag{4}$$

shown by the green triangles in Fig. 3(b). It is historically called a "floating" phase, to do with the appearance of a similar phenomenon in the physics of an incommensurate adsorbent on top of a crystalline substrate [46–48]. The physical picture is that above T_N, the domain walls proliferate along the z direction, destroying the true long-range order and resulting in the incommensurability of the floating phase. The appearance of such a phase in the 2D ANNNI model was originally indicated by mean-field and noninteracting approximations [27,49].

Our analysis shows that the floating phase is separated from the ordered commensurate phase with $\mathbf{Q}_2 = (0, \pi/2)$ [sometimes called the double-column antiferromagnet (DCAF)] by a true phase transition at T_N, at which the degree of incommensurability of the floating phase vanishes as a power law: $q - Q_2 = \Delta q \sim (T - T_N)^{\beta}$ [see Figs. 3(c) and 3(d)]. This transition, first investigated by Pokrovskii and Talapov [50], is expected to have $\beta = 1/2$ in 2D, which is verified by the data collapse of $\Delta q \sim (t)^{0.5}$ for different values of J_{z2} as shown in Fig. 3(d), where $t \equiv [T - T_N(J_{z2})]/T_N(J_{z2})$.

At the upper boundary T_{fl} [dashed line in Fig. 3(a)], the floating phase is separated from the disordered paramagnet [with exponentially decaying correlations, shown by yellow circles in Fig. 3(b)] by a Berezinskii–Kosterlitz–Thouless (BKT) transition [27,51–56]. Algebraic correlations are typically seen only at a critical point, whereas here they are a signature of a phase of matter in the extended temperature range $T_N < T < T_{\text{fl}}$, with the exponent $0 < \eta < 1/4$ varying smoothly as a function of temperature. We determine T_{fl} as the position where the correlation function

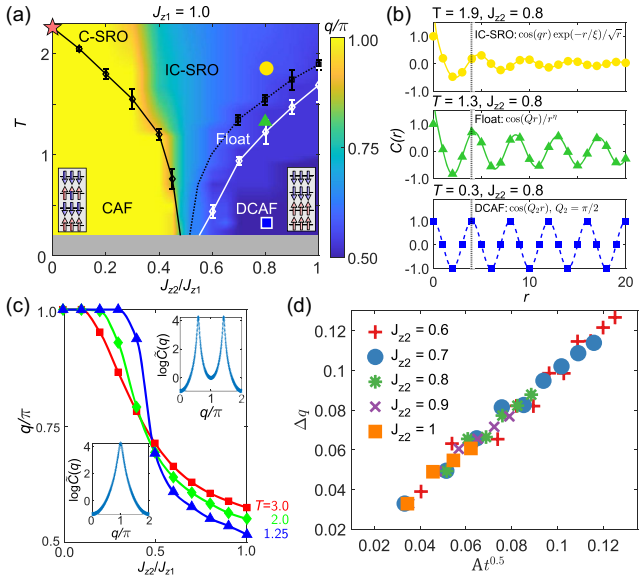

FIG. 3. False color plot (a) indicating the evolution of q. By definition, the Fourier-space correlations $\tilde{C}(\mathbf{q}) \equiv \sum_i e^{-i\mathbf{q}\cdot\mathbf{r}_i} \langle \sigma(0)\sigma(\mathbf{r}_i) \rangle$ are peaked at a wave vector $\mathbf{q} = (0, q)$. Insets in panel (a) illustrate the low-temperature ordered phases. The star on the vertical axis indicates T_N for the nearest-neighbor Ising model [31,57]. (b) Monte Carlo data and analytical fits to the spin correlation function. The vertical dotted line indicates the magnetic period in the DCAF phase. (c) Evolution of q at fixed temperatures as a function of J_{z2}/J_{z1}. The insets (c) depict the single- and double-peak structure of the Fourier-space correlations in the CAF and DCAF phases, respectively. (d) Data collapse of $\Delta q = At^{0.5}$ (where A is a proportionality constant depending on J_{z2}), indicating a second-order phase transition into the DCAF phase at critical temperature T_N with critical exponent $\beta = 0.5$.

fits match the BKT critical exponent $\eta = 0.25$ (see the Supplemental Material [33] for fit data and discussion of finite-size effects). Earlier studies showed that the floating phase boundary $T_{\rm fl}$ may coincide with T_N [51,52]. However, in agreement with more recent studies using complimentary methods [54–56], our results indicate a finite range of algebraic correlations with $0 < \eta < 0.25$ smoothly varying for multiple system sizes [33].

Lifshitz transition.—As the above analysis and Fig. 3(a) illustrate, the wave vector $\mathbf{q}$ characterizing the spatial dependence of the spin correlation function can change as a function of temperature. More generally, $\mathbf{q} = (0, q)$ also changes as a function of the ratio J_{z2}/J_{z1}, as shown in Fig. 3(c), from the commensurate $\mathbf{q} = \mathbf{Q}_1 = (0, \pi)$ in the low-frustrated region [yellow in Fig. 3(a)], to incommensurate at higher frustration. This is known as the *Lifshitz transition* (a misnomer, as it is a crossover in the thermodynamic sense), characterized by the appearance of the double-peak structure in the spin-structure factor $S(\mathbf{q})$, as shown in the inset of Fig. 4. Upon crossing the Lifshitz transition, shown schematically by a dashed gray line in Fig. 4, the wave vector changes continuously away from $\mathbf{q} = \mathbf{Q}_1$ and at high temperatures $\mathbf{q}$ approaches fixed incommensurate values that depend on J_{z2}/J_{z1}. The Lifshitz line T_L can be clearly seen in our Monte Carlo simulations as the line of color gradient separating the yellow region from green-blue in Fig. 3(a). At least in the ANNNI model studied here (and perhaps more generally), the Lifshitz line merges with the boundary of the LRO1 phase upon approaching the maximally frustrated region near $J_{z2} = 0.5$. In addition to the Lifshitz transition, the onset of incommensurate short-range correlations also manifests itself in the real space in a subtle way, via the so-called "disorder transition" [58,59], discussed in the Supplemental Material [33].

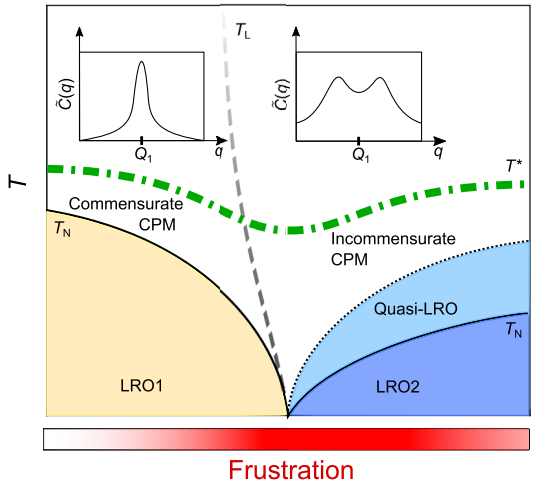

FIG. 4. Schematic phase diagram of a frustrated magnet with two competing orders. The insets depict the spin correlation function $\tilde{C}(q)$, proportional to the static spin structure factor measured in neutron scattering. The quasi-LRO phase with algebraic correlations is specific to the 2D ANNNI model but the other features should apply to generic magnets with frustration and anisotropic interactions.

Discussion.—The present work indicates that a generic temperature-frustration phase diagram looks schematically as depicted in Fig. 4: the two commensurate orders, LRO1 and LRO2, form at the lowest temperatures, characterized by the different (commensurate) ordering wave vectors $\mathbf{q} = \mathbf{Q}_1$ and $\mathbf{Q}_2$, respectively. The melting of these magnetic crystals occurs via an intermediate, generically anisotropic correlated paramagnet, which can be commensurate or incommensurate depending on the strength of frustration in the interactions. Note that the CPM regime identified in the present 2D model corresponds to the "devil's staircase" part of the phase diagram in the originally studied 3D version of the ANNNI model [22–29]. It is reasonable to conclude that the reduced dimensionality amplifies the role of thermal fluctuations, thus destroying the staircase's long-range order in favor of the short-range CPM.

In addition to the study of the CPM, we have confirmed the existence of the floating phase by observing, in order of decreasing temperature, the divergence of the correlation length at $T_{\rm fl}$, an extended temperature range $T_N < T < T_{\rm fl}$ of algebraic correlations with a continuously varying power law, followed by the critical scaling of Δq at T_N [Fig. 3(d)] (See Supplemental Material [33] for additional data). The appearance of this quasi-LRO floating phase in the ANNNI model can be understood as an attempt of a system to form an incommensurate long-range order: true LRO with incommensurate $\mathbf{q}$ is forbidden by classical fluctuations in 2D [27]. There are many layered magnets with Ising anisotropy whose spin correlations can be well approximated to be 2D-like, and the phenomenon of a floating phase—first discussed in statistical mechanics of surface adsorbates [46–48]—ought perhaps to be revisited experimentally.

While the specific model discussed in this work has Ising anisotropy, the appearance of the anisotropic correlated paramagnet above T_N and below some crossover scale T^* (shown schematically by a green line in Fig. 4) is more general. Indeed, it appears ubiquitous in many classical as well as quantum magnets, at elevated temperatures where thermal fluctuations dominate. The appearance of such a CPM phase is often revealed by a slow recovery of the full magnetic entropy at temperatures notably higher than the long-range ordering at T_N, such as that found in, e.g., Eu-based helimagnets [9–11], helimagnetic $CeRhIn_5$, and related heavy fermion compounds [13–15]. The anisotropy of this CPM phase can be directly seen in layered ferromagnets such as CrI_3 and $CrSiTe_3$ by various means, such as neutron scattering [60] and optical polarimetry [16]. Crucially, we found that the dynamical temperature range $\Delta T = (T^* - T_N)$ where the CPM is realized becomes broader with increased frustration (toward the middle of the

horizontal axis in Fig. 4). Indeed, it is in this regime that frustrations can result in a disordered classical spin liquid state, of which classical spin ices such as $Ho_2Ti_2O_7$ and $Dy_2Ti_2O_7$ are famous examples [61]. For quantum magnets, which are beyond the scope of the present work, the interplay of quantum and thermal fluctuations adds to the complexity of the correlated quantum paramagnet phase, which deserves future investigations.

M. A. T. brought experimental motivation for the work. A. H. N. and M. A. T. designed the project, and M. W. B. performed the Monte Carlo simulations and data analysis. All authors contributed to the discussion of the results and writing of the manuscript. The authors acknowledge fruitful discussions with David Huse. M. W. B. and A. H. N. were supported by the Robert A. Welch Foundation, Grant No. C-1818. A. H. N. was also supported by the National Science Foundation Division of Materials Research Grant No. DMR-1917511. The Monte Carlo calculations were performed at the Rice University's Center for Research Computing (CRC), supported in part by the Big-Data Private-Cloud Research Cyberinfrastructure MRI award funded by NSF under Grant No. CNS-1338099. M. A. T. was supported by the U.S. Department of Energy, Office of Basic Energy Sciences, Division of Materials Sciences and Engineering. Ames Laboratory is operated for the U.S. Department of Energy by Iowa State University under Contract No. DE-AC02-07CH11358. A. H. N. acknowledges the hospitality of the Aspen Center for Physics, which is supported by the National Science Foundation Grant No. PHY-1607611.

*nevidomskyy@rice.edu

[1] A. P. Ramirez, Annu. Rev. Mater. Sci. **24**, 453 (1994).
[2] J. S. Gardner, M. J. P. Gingras, and J. E. Greedan, Rev. Mod. Phys. **82**, 53 (2010).
[3] D. A. Huse and A. D. Rutenberg, Phys. Rev. B **45**, 7536 (1992).
[4] P. Mendels and A. S. Wills, in *Introduction to Frustrated Magnetism*, edited by C. Lacroix, F. Mila, and P. Mendels (Springer, New York, 2011), Chap. 9.
[5] J. T. Chalker, in *Introduction to Frustrated Magnetism*, edited by C. Lacroix, F. Mila, and P. Mendels (Springer, New York, 2011), Chap. 1.
[6] L. Savary and L. Balents, Rep. Prog. Phys. **80**, 016502 (2016).
[7] R. Moessner and J. T. Chalker, Phys. Rev. B **58**, 12049 (1998).
[8] G. Misguich and C. Lhuillier, in *Frustrated Spin Systems* (World Scientific, Singapore, 2005), pp. 229–306.
[9] N. S. Sangeetha, S. Pakhira, D. H. Ryan, V. Smetana, A.-V. Mudring, and D. C. Johnston, Phys. Rev. Mater. **4**, 084407 (2020).
[10] N. S. Sangeetha, E. Cuervo-Reyes, A. Pandey, and D. C. Johnston, Phys. Rev. B **94**, 014422 (2016).
[11] S. Pakhira, M. A. Tanatar, and D. C. Johnston, Phys. Rev. B **101**, 214407 (2020).
[12] M. A. Tanatar, N. S. Sangeetha, S. Pakhira, M. W. Butcher, A. H. Nevidomskyy, D. C. Johnston, and R. Prozorov (unpublished).
[13] H. Hegger, C. Petrovic, E. G. Moshopoulou, M. F. Hundley, J. L. Sarrao, Z. Fisk, and J. D. Thompson, Phys. Rev. Lett. **84**, 4986 (2000).
[14] J. Paglione, M. A. Tanatar, D. G. Hawthorn, R. W. Hill, F. Ronning, M. Sutherland, L. Taillefer, C. Petrovic, and P. C. Canfield, Phys. Rev. Lett. **94**, 216602 (2005).
[15] E. D. Bauer, H. O. Lee, V. A. Sidorov, N. Kurita, K. Gofryk, J.-X. Zhu, F. Ronning, R. Movshovich, J. D. Thompson, and T. Park, Phys. Rev. B **81**, 180507(R) (2010).
[16] A. Ron, E. Zoghlin, L. Balents, S. D. Wilson, and D. Hsieh, Nat. Commun. **10**, 1654 (2019).
[17] J. Paglione, M. A. Tanatar, D. G. Hawthorn, E. Boaknin, R. W. Hill, F. Ronning, M. Sutherland, L. Taillefer, C. Petrovic, and P. C. Canfield, Phys. Rev. Lett. **91**, 246405 (2003).
[18] J. Paglione, M. A. Tanatar, D. G. Hawthorn, F. Ronning, R. W. Hill, M. Sutherland, L. Taillefer, and C. Petrovic, Phys. Rev. Lett. **97**, 106606 (2006).
[19] M. A. Tanatar, J. Paglione, C. Petrovic, and L. Taillefer, Science **316**, 1320 (2007).
[20] R. J. Elliott, Phys. Rev. **124**, 346 (1961).
[21] J. Rossat-Mignod, P. Burlet, J. Villain, H. Bartholin, W. Tcheng-Si, D. Florence, and O. Vogt, Phys. Rev. B **16**, 440 (1977).
[22] J. von Boehm and P. Bak, Phys. Rev. Lett. **42**, 122 (1979).
[23] P. Bak and J. von Boehm, Phys. Rev. B **21**, 5297 (1980).
[24] M. E. Fisher and W. Selke, Phys. Rev. Lett. **44**, 1502 (1980).
[25] W. Selke and M. E. Fisher, Z. Phys. B **40**, 71 (1980).
[26] P. Bak, Phys. Rev. Lett. **46**, 791 (1981).
[27] P. Bak, Rep. Prog. Phys. **45**, 587 (1982).
[28] M. Pleimling and M. Henkel, Phys. Rev. Lett. **87**, 125702 (2001).
[29] A. K. Murtazaev and Z. G. Ibaev, Low Temp. Phys. **35**, 792 (2009).
[30] P. Weiss, J. Phys. Theor. Appl. **6**, 661 (1907).
[31] L. Onsager, Phys. Rev. **65**, 117 (1944).
[32] N. D. Mermin and H. Wagner, Phys. Rev. Lett. **17**, 1133 (1966).
[33] See Supplemental Material at http://link.aps.org/supplemental/10.1103/PhysRevLett.130.166701 for additional technical details on the Monte Carlo method, finite-size effects, and the Lifshitz and disorder transitions. This material includes additional Refs. [34–43].
[34] U. Wolff, Phys. Rev. Lett. **62**, 361 (1989).
[35] E. Luijten and H. W. Blöte, Int. J. Mod. Phys. C **06**, 359 (1995).
[36] R. H. Swendsen and J.-S. Wang, Phys. Rev. Lett. **57**, 2607 (1986).
[37] E. Marinari and G. Parisi, Europhys. Lett. **19**, 451 (1992).
[38] K. Hukushima and K. Nemoto, J. Phys. Soc. Jpn. **65**, 1604 (1996).
[39] E. Granato, Phys. Rev. B **85**, 054508 (2012).
[40] J. M. Kosterlitz and D. J. Thouless, J. Phys. C **6**, 1181 (1973).
[41] J. M. Kosterlitz, J. Phys. C **7**, 1046 (1974).

[42] U. Schollwöck, T. Jolicœur, and T. Garel, Phys. Rev. B **53**, 3304 (1996).
[43] J. H. Pixley, A. Shashi, and A. H. Nevidomskyy, Phys. Rev. B **90**, 214426 (2014).
[44] M. Campanino, D. Ioffe, and Y. v. Velenik, Probab. Theory Relat. Fields **125**, 305 (2003).
[45] E. W. Montroll, R. B. Potts, and J. C. Ward, J. Math. Phys. (N.Y.) **4**, 308 (1963).
[46] S. N. Coppersmith, D. S. Fisher, B. I. Halperin, P. A. Lee, and W. F. Brinkman, Phys. Rev. Lett. **46**, 549 (1981).
[47] S. N. Coppersmith, D. S. Fisher, B. I. Halperin, P. A. Lee, and W. F. Brinkman, Phys. Rev. B **25**, 349 (1982).
[48] M. E. Fisher and D. S. Fisher, Phys. Rev. B **25**, 3192 (1982).
[49] A. Finel and D. de Fontaine, J. Stat. Phys. **43**, 645 (1986).
[50] V. L. Pokrovskii and A. L. Talapov, Zh. Eksp. Teor. Fiz. **78**, 269 (1980) [Sov. Phys. JETP **51**, 134 (1980)].
[51] T. Shirahata and T. Nakamura, Phys. Rev. B **65**, 024402 (2001).
[52] A. K. Chandra and S. Dasgupta, J. Phys. A **40**, 6251 (2007).
[53] A. K. Chandra and S. Dasgupta, Phys. Rev. E **75**, 021105 (2007).
[54] M. Beccaria, M. Campostrini, and A. Feo, Phys. Rev. B **76**, 094410 (2007).
[55] T. Shirakura, F. Matsubara, and N. Suzuki, Phys. Rev. B **90**, 144410 (2014).
[56] Y. Hu and P. Charbonneau, Phys. Rev. B **103**, 094441 (2021).
[57] H. A. Kramers and G. H. Wannier, Phys. Rev. **60**, 252 (1941).
[58] J. Stephenson, Can. J. Phys. **47**, 2621 (1969).
[59] J. Stephenson, J. Math. Phys. (N.Y.) **11**, 420 (1970).
[60] L. Chen, J.-H. Chung, B. Gao, T. Chen, M. B. Stone, A. I. Kolesnikov, Q. Huang, and P. Dai, Phys. Rev. X **8**, 041028 (2018).
[61] S. T. Bramwell and M. J. P. Gingras, Science **294**, 1495 (2001).